EARTH SCIENCES

# Ten-year seasonal climate reforecasts over South America using the Eta Regional Climate Model

SIN CHAN CHOU, CLAUDINE DERECZYNSKI, JORGE LUÍS GOMES,
JOSÉ FERNANDO PESQUERO, ANA MARIA H. DE AVILA, NICOLE C. RESENDE,
LUÍS FELIPE ALVES, RAMIRO RUIZ-CÁRDENAS, CARLOS RENATO DE SOUZA &
JOSIANE FERREIRA F. BUSTAMANTE

**Abstract:** Ten-year seasonal climate reforecasts over South America are obtained using the Eta Regional Climate Model at 40 km resolution, driven by the large-scale forcing from the global atmospheric model of the Center for Weather Forecasts and Climate Studies. The objective of this work is to evaluate these regional reforecasts. The dataset is comprised of four-month seasonal forecasts performed on a monthly basis between 2001 and 2010. An ensemble of five members is constructed from five slightly different initial conditions to partially reduce the uncertainty in the seasonal forecasts. The seasonal mean precipitation and 2-meter temperature forecasts are compared with the observations. The comparison shows that, in general, forecasted precipitation is underestimated in the central part of the continent in the austral summer, whereas the forecasted 2 meter temperature is underestimated in most parts of the continent and throughout the year. Skill scores show higher skill in the northern part of the continent and lower skill in the southern part of the continent, but mixed skill signs are seen in the central part of the continent. During the El Niño and La Niña seasons, the forecast skill scores clearly increase. The downscaling of the Eta model seasonal forecasts provides added value over the driver global model forecasts, especially during rainy periods.

**Key words:** Seasonal forecasts, Regional Climate Model, Eta model, South America, forecast skill, added value.

## INTRODUCTION

The information derived from seasonal-timescale climate predictions is extremely relevant for planning actions in various sectors of society, particularly in the energy sector, where seasonal rainfall forecasts could support activities related to the generation, transmission, and distribution of energy. For example, if the exceptional drought of 2014/2015 in southeastern Brazil (Otto et al. 2015) had been predicted some months in advance, the Brazilian government could have been prepared for the drier than usual season.

It is known that individual weather patterns cannot be predicted beyond a period of approximately two weeks because of the nonlinear dynamics of the atmosphere that limit predictability beyond individual synoptic events (Lorenz 1982). However, the predictability of the mean climate in certain regions and seasons increases from the lower boundary forcing (Shukla 1998, Rodwell & Doblas-Reyes, 2006, Brankovic et al. 1994), which evolves much

more slowly over longer timescales. In tropical regions, where circulation is mostly determined by the Hadley and Walker cells, and because the fluctuations in these cells are strongly dependent on the sea-surface temperature, the predictability is potentially superior to that of the rest of the world (Palmer & Anderson 1994, Shukla 1998, Kumar 2007, Kumar et al. 2007, Barnston et al. 2010).

Seasonal forecasts from global climate models (GCMs) generally provide information at resolutions that are still too coarse for planning or for taking actions at a local scale. The use of very high-resolution GCMs is still limited by computational resources. Therefore, the application of dynamical downscaling (Laprise et al. 2000) may provide more detailed information for seasonal climate impact studies. In the dynamical downscaling technique, a regional climate model (RCM) is nested into a GCM. The global model provides the initial, lateral and lower boundary conditions, which contain information about the large-scale atmospheric circulation. On the other hand, the regional model reproduces the aspects of regional scale at high resolution. In addition, the higher resolution of the RCMs allows more robust circulation and a better description of the surface conditions, which provides added value over the driver coarse resolution model simulations (Laprise et al. 2008).

The use of RCMs to generate long-term forecasts has been attempted since the work by Dickinson et al. (1989). Giorgi (1990), Misra et al. (2003), Liang et al. (2006), among others, produced seasonal integrations and demonstrated the potential of RCMs for reproducing climate variability. The first attempt to explore the dynamical downscaling technique over South America was carried out by Chou et al. (2000), who performed and evaluated a one-month long simulation with the aim of exploring

the quality of extended range forecasts by nesting the Eta RCM into the Center for Weather Forecasts and Climate Studies (in Portuguese "Centro de Previsão de Tempo e Estudos Climáticos" – CPTEC) of the National Institute for Space Research (in Portuguese "Instituto Nacional de Pesquisas Espaciais" - INPE) GCM. Following Chou et al. (2000); Menéndez et al. (2001), Nicolini et al. (2002), and Misra et al. (2002) demonstrated that the ensemble of the Eta model was able to improve over the driving GCM behavior for reproducing the observed climate anomalies and, consequently, these authors highlighted that the use of RCMs nested into GCMs was a useful tool for the purpose of climate prediction. In a recent review by Ambrizzi et al. (2019), the authors provided a timeline of RCM studies over South America, including a list of a few seasonal forecast experiments for the region, which were carried out over the last 13 years using either the Eta or the RegCM models. In all cases, the RCM was driven by the INPE's GCM. The authors highlighted that the seasonal forecast using RCMs is still in development in the region.

The use of seasonal forecasts to drive impact models in key areas, such as hydrology and agriculture, requires improvements. One possible way to improve forecast quality is to adjust the forecast model output based on a database of retrospective forecasts (reforecasts) from the same model, as indicated by Hamill et al. (2004). These authors showed that the reforecasts provide statistical measures and properties of the forecast system, such as the anomaly correlations, the systematic errors, and the forecast skill. The reforecasts represent the model climatology at the forecast range. Rajagopalan et al. (2002), Stefanova & Krishnamurti (2002), Hamill (2012), Pegion & Kumar (2013) used multimodel reforecasts to improve seasonal predictions.

At INPE, the regional Eta model (Chou 1996, Chou et al. 2005, Mesinger et al. 2012) has been applied for weather and climate forecasts. Evaluations of extended and seasonal forecasts that range over South America (Chou et al. 2000, 2002, 2005) have shown the improvement of the Eta model over the driver CPTEC/INPE global model forecasts (Cavalcanti et al. 2002). The seasonal forecasts using the Eta model over South America have shown the model's ability to reproduce seasonal variability (Bustamante J.F., unpublished data). A comparison between the Eta model seasonal forecasts driven by CPTEC AGCM and driven by the CPTEC coupled Ocean-Atmosphere General Circulation Model (Pilotto et al. 2012) showed that the latter reduces the error in precipitation forecasts over the intertropical convergence zone. The updated version of the Eta model (Mesinger et al. 2012) replaced the previous version of the model for seasonal forecasts (Chou et al. 2005). The major changes in the current version of the model lie in the vertical advection scheme, which converts the model into a fully finite volume, and the 'cut-cell' refinement of the eta vertical coordinate, which may intensify downslope windstorms. Simulations using the Eta model over seasonal time ranges (Resende & Chou 2015) driven by CFSR reanalyses (Saha et al. 2010) showed that the model exhibits a cold bias from near the surface up to the upper levels of the model atmosphere. Ferreira & Chou (2018) evaluated the seasonal simulations from the Eta model and demonstrated that the model has some skill for simulating climatic extremes.

The objective of this work is to evaluate the seasonal forecasts from the Eta Regional Climate Model over the South and Central American regions. The evaluation is based on identifying the systematic errors and the skill scores of the seasonal forecasts on a monthly basis. The model performance during extreme events is also evaluated. This work provides information on the performance of the operational seasonal forecasts produced by the Eta model for the South and Central American regions. The information on the forecast skills, discriminated by the time of the year and by locations, is a necessary step before the application of these forecasts to various socioeconomic sectors.

## MATERIALS AND METHODS

In this section, the model description is provided. The evaluation of seasonal forecasts is based on identifying the systematic errors in the precipitation and temperature forecasts.

### Eta model description

The Eta is a grid-point model originally developed in the University of Belgrade and the former Yugoslav Hydrometeorological Service (Mesinger et al. 1988). The model was operational at the National Centers for Environmental Prediction (Black 1994) and became operational at the end of 1996 at the Center for Weather Forecasts and Climate Studies (CPTEC) of the Brazilian National Institute for Space Research (INPE) (Chou 1996). The model has produced operationally seasonal forecasts since 2001 over the South American domain with 40 km horizontal resolution.

The surfaces of the model vertical coordinates, the eta coordinate (Mesinger 1984), are approximately horizontal, which is a characteristic that makes the model suitable for use in regions with steep orography, such as the Andes Mountains. Seluchi et al. (2003) demonstrated the ability of the model to simulate downslope windstorms near the Andes. The refinement of the coordinates around mountains (Mesinger et al. 2012), the so-called "cut-cells", has been an additional improvement to simulate the major windstorms in the Andes (Antico et al. 2017).

The model horizontal grid adopts the semi-staggered Arakawa E-grid. The time-difference scheme uses a modified forward-backward numerical scheme (Mesinger F., unpublished data, Janjic 1979), and the space difference adopts the Arakawa approach with energy conservation in the transformation between potential and kinetic energy (Janjic 1984, Mesinger et al. 1988). The lateral boundary conditions are treated by the Mesinger (1977) scheme, which prescribes the driver model state variables in the single outermost row in the inflow points and extrapolates tangential velocity components at the outflow points. No relaxation is applied anywhere in the model domain.

The current version uses the Betts-Miller scheme (Betts & Miller 1986; Janjic 1994) as the cumulus parameterization scheme. Grid-scale precipitation is produced by the Zhao scheme (Zhao et al. 1997). Radiation schemes come in a package developed by the Geophysical Fluid Dynamics Lab that treats shortwave fluxes with the Lacis and Hansen (1974) scheme and longwave fluxes with the Schwarzkopf and Fels (1991) scheme. The land-surface scheme uses the NOAH (Ek et al. 2003) scheme. The surface layer is based on the Monin-Obukhov similarity theory and uses the Paulson (1970) stability

functions. The atmospheric turbulence uses Mellor-Yamada closure of 2.5 level. The current version contains the updates described in Mesinger et al. (2012).

The model domain covers South America, Central America and the adjacent oceans (Figure 1). The model resolution is approximately 40 km in the horizontal direction and consists of 38 layers in the vertical direction. The integration period is 4.5 months and approximately the initial fifteen days are discarded. Therefore, the seasonal forecasts are presented as 4-month forecast ranges. To consider the uncertainty of the forecasts, the ensemble is constructed from initial conditions by starting on days 13, 14, 15, 16, and 17 of the month before the forecast period. For example, for the forecast of February, March, April, and May, the ensemble of forecasts start on days 13, 14, 15, 16, and 17 of January. These runs are driven by the CPTEC global climate atmospheric model (Cavalcanti et al. 2002) at T62L28 resolutions through the initial and lateral boundary conditions. The RCM runs are synchronized with the global model, with both models starting on the same dates. The lateral boundary conditions are updated every 6 hours. The lower boundary conditions consist of sea surface temperature
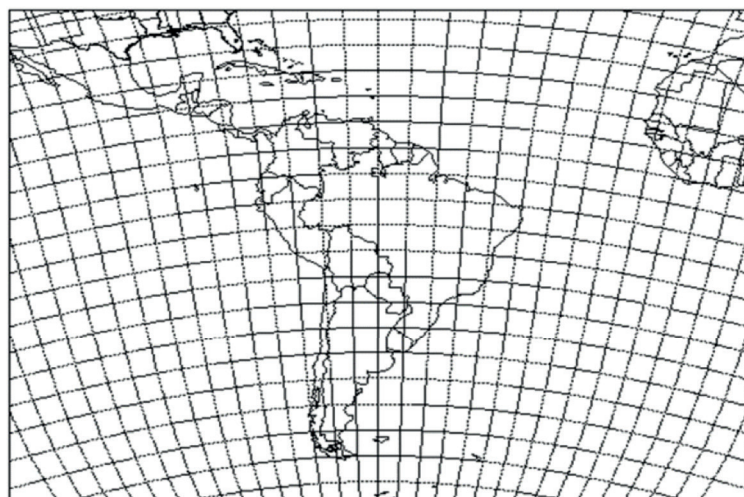


**Figure 1.** 40-km Eta RCM domain centered in South America.

(SST) and land surface conditions. Sea surface temperature is consistent with the global model run, which adopts the observed SST as the initial condition and persists the SST anomaly of the initial condition throughout the integration. Therefore, a constant SST anomaly is added to the climatological SST, which provides seasonal variability to the SST field during the integration period. Soil moistures and temperatures are taken from climatological data. The seasonal reforecasts are constructed for the period from 2001 to 2010, of monthly reforecasts of 4.5 months length, and five members integrated from different initial conditions as described above.

### Forecast evaluation

Evaluations of the seasonal forecasts are based on the monthly means and skill scores of precipitation and temperature forecasts.

The skill scores consist of the temporal correlation of seasonal precipitation anomalies between the seasonal forecasts and the *Global Precipitation Climatology Project* (GPCP) dataset (Huffman et al. 1997). The precipitation anomaly is calculated with respect to the mean of the period between 2001 and 2010. To evaluate the five-member ensemble, five temporal correlations of precipitation anomalies (one for each different initial date) are calculated. Then, a mean value of the temporal correlation is calculated from the five different seasonal precipitation anomaly correlations. Therefore, a single value of the metric is assigned to each season at each grid point. The skills of the forecasts with lead times of one and two months are calculated.

For model evaluation, 2 meter temperature forecasts are compared against observations derived from the Climate Research Unit (CRU) dataset (Mitchell & Jones 2005), and the

lower-level winds are compared against Era-Interim reanalyses (Dee et al. 2011).

## RESULTS

Seasonal forecasts are generally reported as three-month anomaly forecasts. Because the model forecast length is 4.5 months, the three-month forecasts can be comprised of the first three months or the last three months of the integration period, which correspond to the one-month or two-month lead times.

### Seasonal mean

It is important to evaluate the model simulations in terms of the seasonal climate variabilities and the spatial patterns of the precipitation forecasts. Figure 2 shows the seasonal mean precipitation forecast produced by the 40 km Eta RCM. The mean value is calculated from the five members of the ensemble and the ten-year period of one-month lead time of each trimester forecast. That is, the seasonal mean value is taken from 50 seasonal forecasts. Each season is identified by the initial letters of the three months in the season, for example, JFM stands for the January-February-March season.

Seasonal precipitation forecasts produced by the Eta model show good agreement with the observational data, according to some known and established precipitation features in the South American region. A major feature of the seasonal variability captured by the forecasts is the band known as the South Atlantic convergence zone, SACZ, which occurs during summer, DJF, and extends from the Amazon region toward southeastern Brazil and over the adjacent Atlantic Ocean (Kodama 1992). During winter, in JJA, precipitation is almost absent in the central part of the continent. In this season, the predicted precipitation is mostly found in the
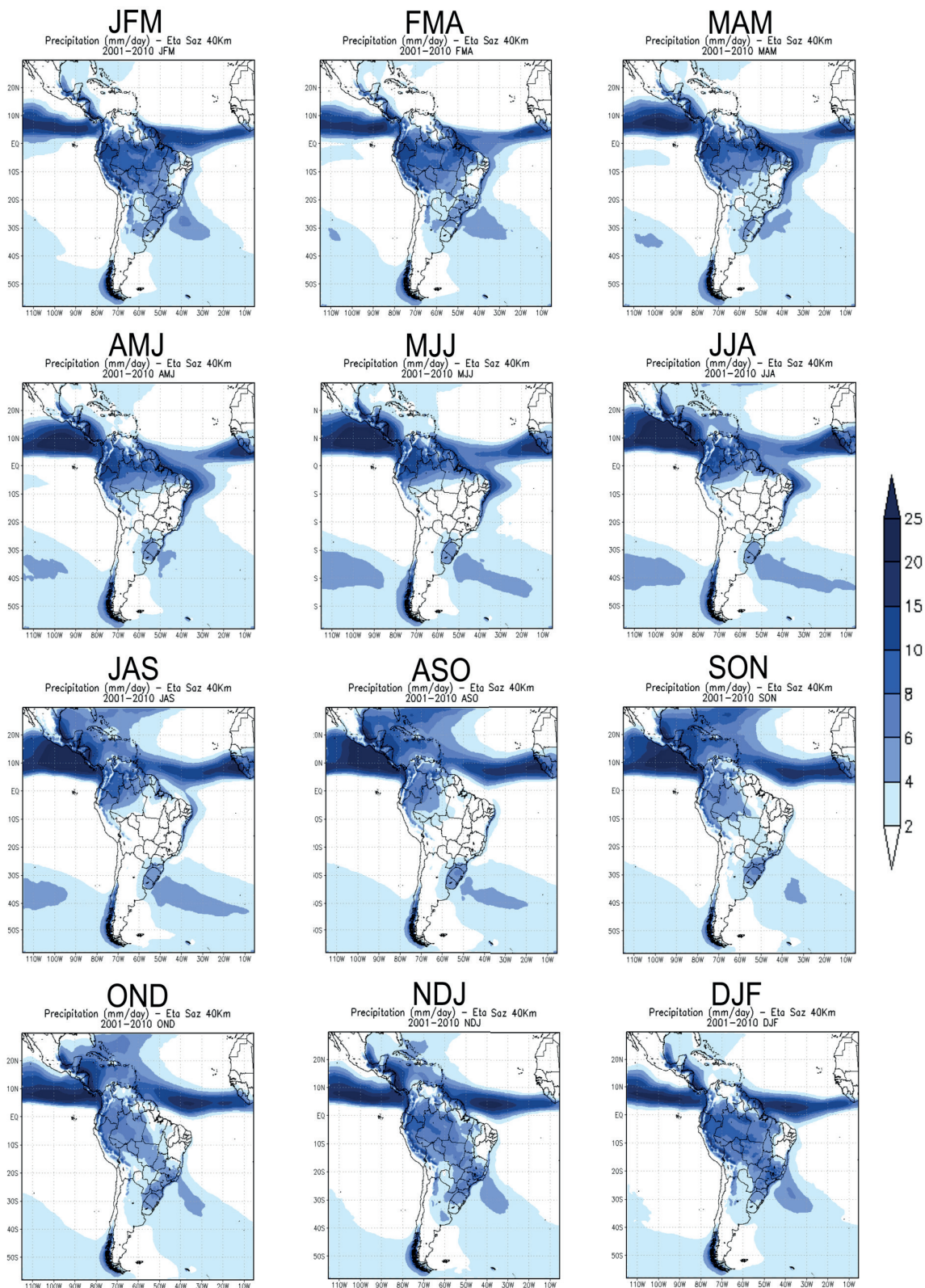
**Figure 2. Seasonal mean precipitation (mm day$^{-1}$) forecast by the Eta Regional Climate Model, averaged over the period 2001-2010 and the five ensemble members.**

northern part of the Amazon basin, and along the northeast coast of Brazil, where easterly disturbances from the Atlantic Ocean reach the coast. These features agree with observations (Yamazaki and Rao 1977). In the southern part of Brazil, the predicted precipitation shows little variability during the year, which is also in agreement with observations. The predicted seasonal precipitation band related to the intertropical convergence zone (ITCZ) migrates in the latitudinal direction through the seasons, in agreement with GPCP observational locations.

Therefore, the model shows reasonable performance in reproducing variations in the spatial patterns of precipitation throughout the seasons. However, the forecast may contain systematic and random errors. Systematic errors generally vary across the seasons as they may be produced by some prevailing weather phenomena that the model fails to correctly capture. Figure 3 shows the systematic model errors in terms of the mean error for each season. The mean error is obtained as the difference between the mean model seasonal precipitation and the GPCP ten-year climatology for the same period as the forecasts. Along the ITCZ band, precipitation amounts are excessive in the reforecasts, particularly over the Pacific Ocean, during the northern hemisphere summer months. This overestimate of precipitation along the ITCZ band extends toward the Caribbean region, and it is larger during the ASO and SON seasons. This error along the ITCZ band may be related to the SST, since these seasonal forecasts used a persistent SST anomaly during the integration.

Pilotto et al. (2012) compared Eta seasonal forecasts nested into CPTEC AGCM and CGCM for the DJF season. These authors demonstrated that the overestimates of precipitation along the ITCZ are generally reduced when the Eta RCM is driven by the SST forecasted by the CPTEC CGCM.

In contrast to the errors over the ocean, seasonal precipitation forecasts in the central part of the continent are generally underestimated throughout the rainy season, which starts in October and ends in March. Off the east coast of northeastern Brazil, the forecasts underestimate the seasonal precipitation during the entire year but more strongly between AMJ and JJA, which is the rainy season for this region. Over the inner continental areas of northeastern Brazil, the seasonal forecasts generally underestimate the precipitation, particularly during FMAM. Similarly, over the continental areas of Central America and the Caribbean, precipitation is underestimated in the seasons between MJJ and SON. In conclusion, the model shows a systematic underestimate of precipitation over continental areas during the rainy season.

As the forecast length is 4.5 months, the forecasts for seasons of three months can be formed as one-month lead time or two-month lead time forecasts. The question addressed here is: does the error pattern change with the forecast lead time? Users may prefer to base their actions on the first or on the second three-month period of the Eta RCM seasonal forecasts. Therefore, for the season DJF, the one-month lead-time forecast runs start in November, whereas for the two-month lead-time the forecast runs starts in October. Figures 4a and 4b show the precipitation forecast errors for two-month lead time for the JJA and DJF seasons. These figures can be compared with Figures 3f and 3l. Comparison between the two forecast lead times shows that, in general, the errors are smaller in the one-month lead forecasts. This result is not obvious because it is generally expected to allow more time for the model soil moisture to develop conditions to reach an equilibrium with the precipitation and the other model physics variables. These results show that, for the Eta RCM, the first months of
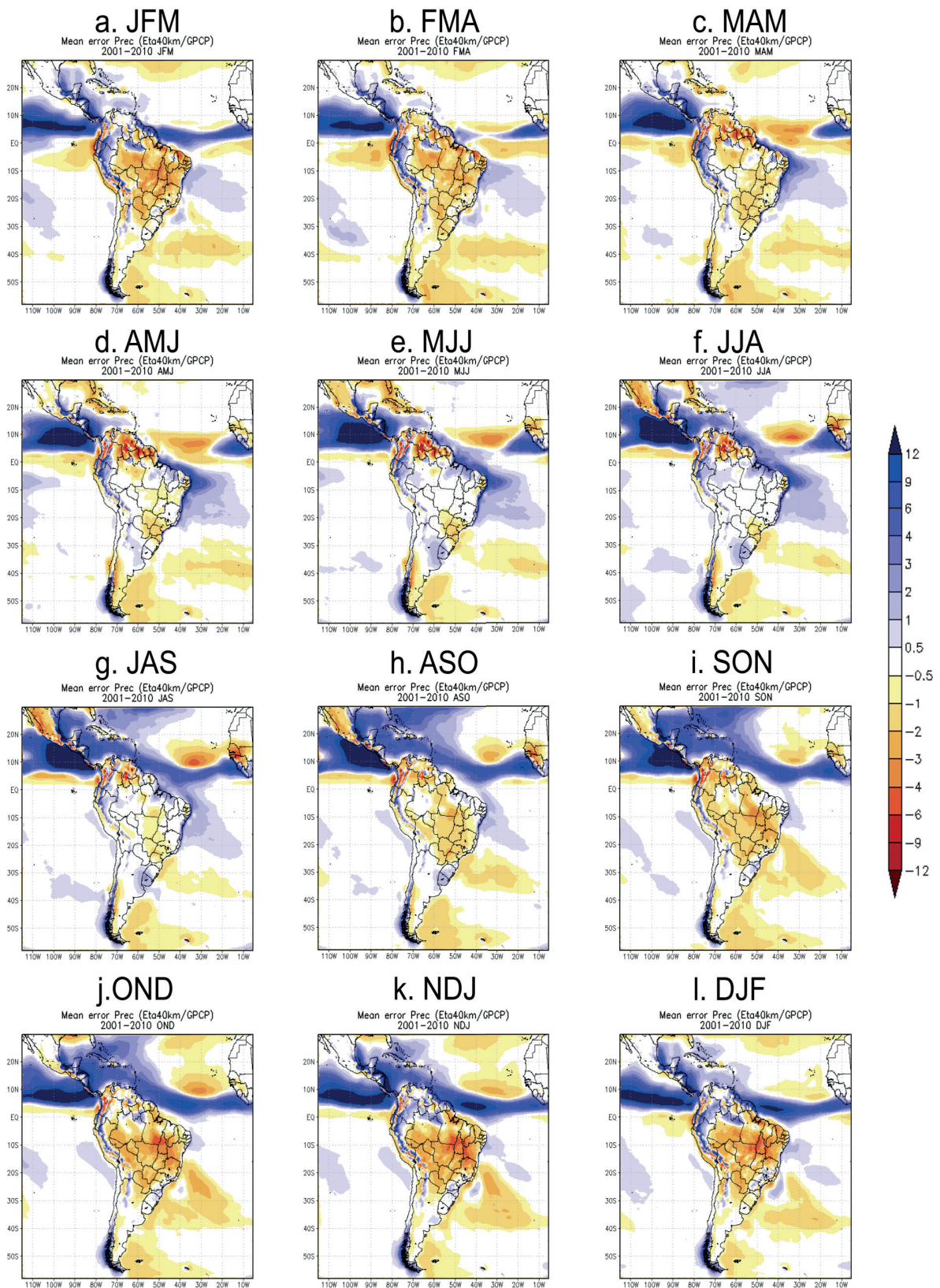
**Figure 3.** Mean errors of seasonal precipitation (mm/3 months) for one-month lead time forecasts.

the seasonal forecasts, the precipitation forecast errors are generally smaller. However, in an operational suite, other forecasts may need to be produced first; therefore the two-month lead forecasts may provide a more useful forecast range.

Temperature error is obtained as the difference between the Eta RCM forecasts and the CRU observations, which are only available over the continent. The seasonal mean temperature forecast errors show a systematic cold bias over most of the continental area (Figure 5), which includes Central and South America. However, warm temperature biases are also seen in the southeastern South America region, mainly in transition seasons, between MAM and MJJ, and in central Brazil between the SON and OND seasons.

The upper levels of the atmosphere also show this cold bias. These temperature errors were also found in the long-term multidecadal simulations (Pesquero et al. 2009, Chou et al. 2012, 2014). This cold bias may be related to the upper levels of the model troposphere, where the underestimation of precipitation

may lead to insufficient latent heat release and, consequently, to less warming at upper levels. This cold bias may also be related to the surface conditions, in the case these conditions do not favor deep convection triggering, as stated by Resende & Chou (2015). Increases in precipitation production should reduce the negative biases in both precipitation and temperature through the additional release of latent heat.

The features of the large-scale flow are evaluated by the 250 hPa winds (Figure 6) and 850 hPa winds (Figure 7). The major circulation features at 250 hPa are present in DJF, such as the anticyclone centered over Bolivia and the cyclonic vortex centered over the northeast coast of Brazil. The Bolivian high is generally related with continental convection and the South Atlantic Convergence Zone (Satyamurty et al. 1998), whereas the trough over the northeastern Brazil is due to the conservation of absolute vorticity of the southerly flow east of the Bolivian High (Kousky & Gan 1981). However, the shape of the vortices shows some differences. The forecast exhibits shorter wavelengths than the Era-Interim reanalysis data. This phenomenon
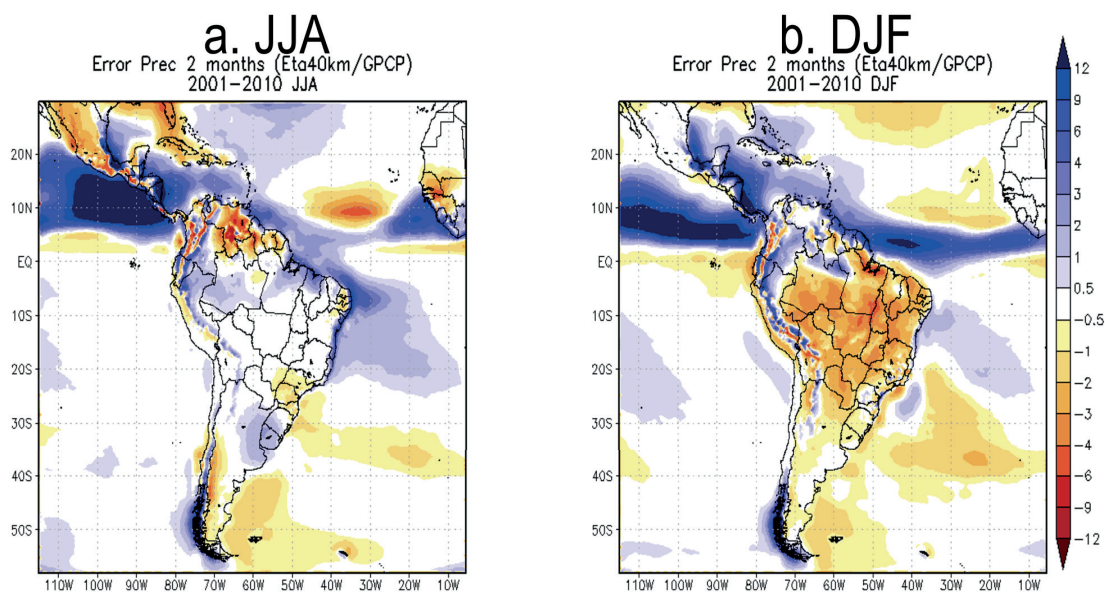


**Figure 4.** Eta RCM seasonal precipitation forecast errors (mm day$^{-1}$) for (a) JJA and (b) DJF, from the two-month lead forecasts.
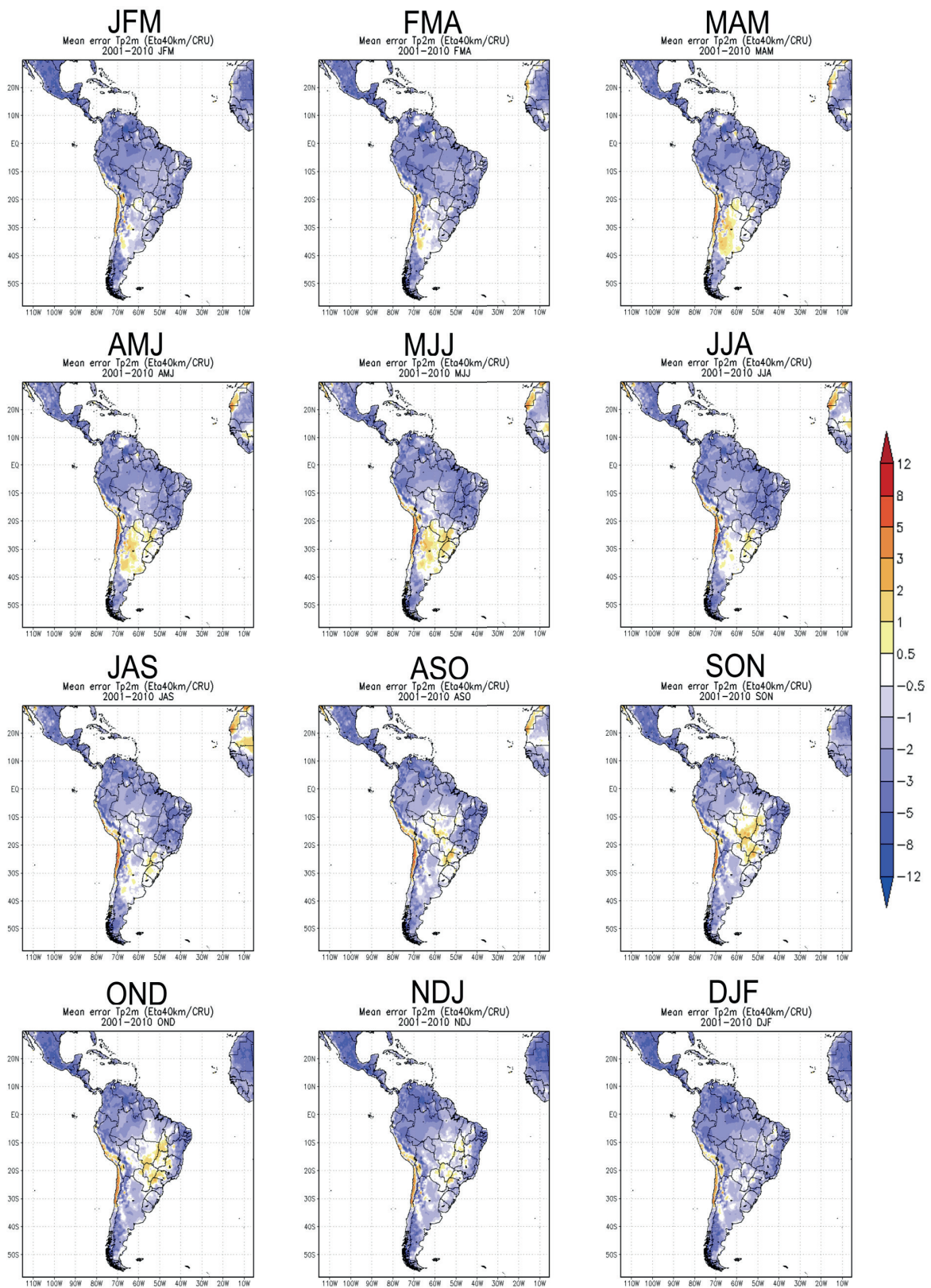
**Figure 5.** Seasonal 2-meter temperature errors (°C), average from 2001-2010 and five ensemble members.

is probably because the latter dataset has a relatively coarser spatial resolution. During the austral winter, the Southern Hemisphere westerlies are represented in the forecasts but, in general, their strength is overestimated.

The Eta model lower tropospheric circulation features (Figure 7), such as the Atlantic and Pacific Anticyclones, and the DJF northerly east of the Andes, are in agreement with the Era-Interim reanalysis in terms of position and intensity in both seasons, DJF and JJA.

## Precipitation skill score

As a measure of the skill of the interannual variability of seasonal precipitation anomaly, skill scores are calculated as the temporal correlation between the forecasted and the observed seasonal precipitation anomaly of the three-month season (e.g., January to March, JFM; February to April, FMA) (Shukla et al. 2000, Sooraj et al. 2012). The scores are shown for one-month (Figure 8) and two-month (Figure 9) lead-time forecasts. In addition, the scores are averaged over the five members of the ensemble. In

general, the skill scores are higher for the one-month lead-time than for the two-month lead-time. It is interesting to show the skill score for both lead times, as the user may also make use of the two-month lead forecast time for advance planning.

Over the northern part of the continent, the NDJ, DJF, and JFM seasons show the highest skills, whereas the FMA, MAM, AMJ, and JJA seasons show moderate skill values; and the JAS, ASO, SON, and OND seasons show the lowest skills. Over the northeastern Brazil, the highest skill scores occur during the MAM, AMJ, and MJJ seasons, which are mostly the rainy period of the region. The central part of Brazil and southeastern Brazil show mixed signs along the year, which indicates low skills for seasonal forecasts. Both, the central and southeastern parts of Brazil shows weak positive scores for the one-month lead time forecasts in the SON, OND, and NDJ seasons, and positive scores for the two-month lead time forecasts in the OND, NDJ, and DJF seasons (Figure 8b).
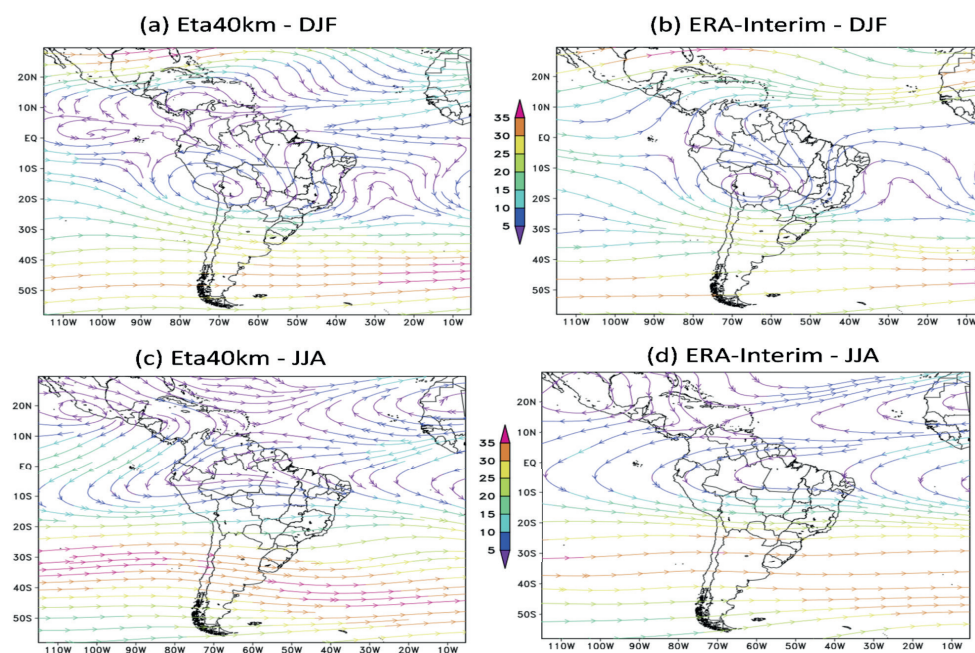


**Figure 6.** 250-hPa mean winds (m s$^{-1}$) for DJF and JJA, (a, c) forecast and (b, d) ERA-Interim reanalysis. The color bars refer to the wind speed.
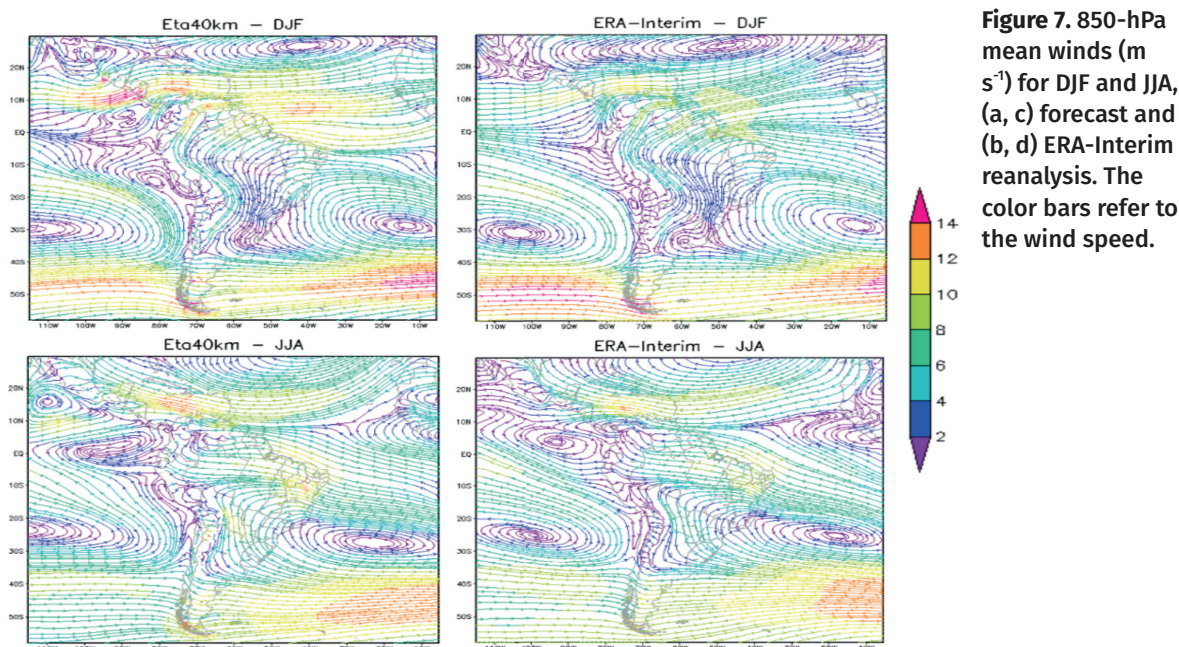
**Figure 7.** 850-hPa mean winds (m s$^{-1}$) for DJF and JJA, (a, c) forecast and (b, d) ERA-Interim reanalysis. The color bars refer to the wind speed.

Over southern parts of South America, signs are mixed, and no clear skill can be concluded from the scores. On the other hand, in Venezuela and Colombia, as well as in the area to the west of the Andes Cordillera, skill scores are positive from the SON season until the JFM season, with score values exceeding 80% at times. Over Central America, the scores are higher between AMJ and JAS (the beginning and the end of the first peak of the rainy season, respectively), although in the Panama region, the scores are generally negative, which means that the forecasted anomaly has a sign opposite to the observed anomaly. These negative values of the skill scores indicate model difficulty for seasonal precipitation forecasts in that region. Southern Mexico exhibited clear high skill scores from NDJ until JFM.

In general, the seasonal precipitation skill scores of the Eta RCM forecasts show higher values in the tropical part of South America but lower values around southern Brazil and Uruguay. The tropical region is known as a region of higher predictability, whereas the southern region is known to exhibit moderate predictability. This skill is in agreement with the driver model skill (Cavalcanti et al. 2002).

Defining reproducibility as the spread among ensemble members, Stern & Miyakoda (1995) showed that in the equatorial regions, especially over the Pacific, the best reproducibility on the globe occurs. Misra et al. (2003), using the Regional Spectral Model (RSM) developed at the National Centers for Environmental Prediction (NCEP), computed a normalized standard deviation to compare and contrast two models (regional and global), showing that the summer season precipitation over tropical and subtropical South America is highly unreproducible in both models.

Although some studies have shown moderate predictability over southeastern South America (SESA) during summer (Coelho et al. 2006), the Eta seasonal precipitation forecasts show higher skills during the rainy season, but low skills during winter. In general, the two-month lead-time forecasts (Figure 9) show slightly lower scores than the one-month lead-time forecasts.
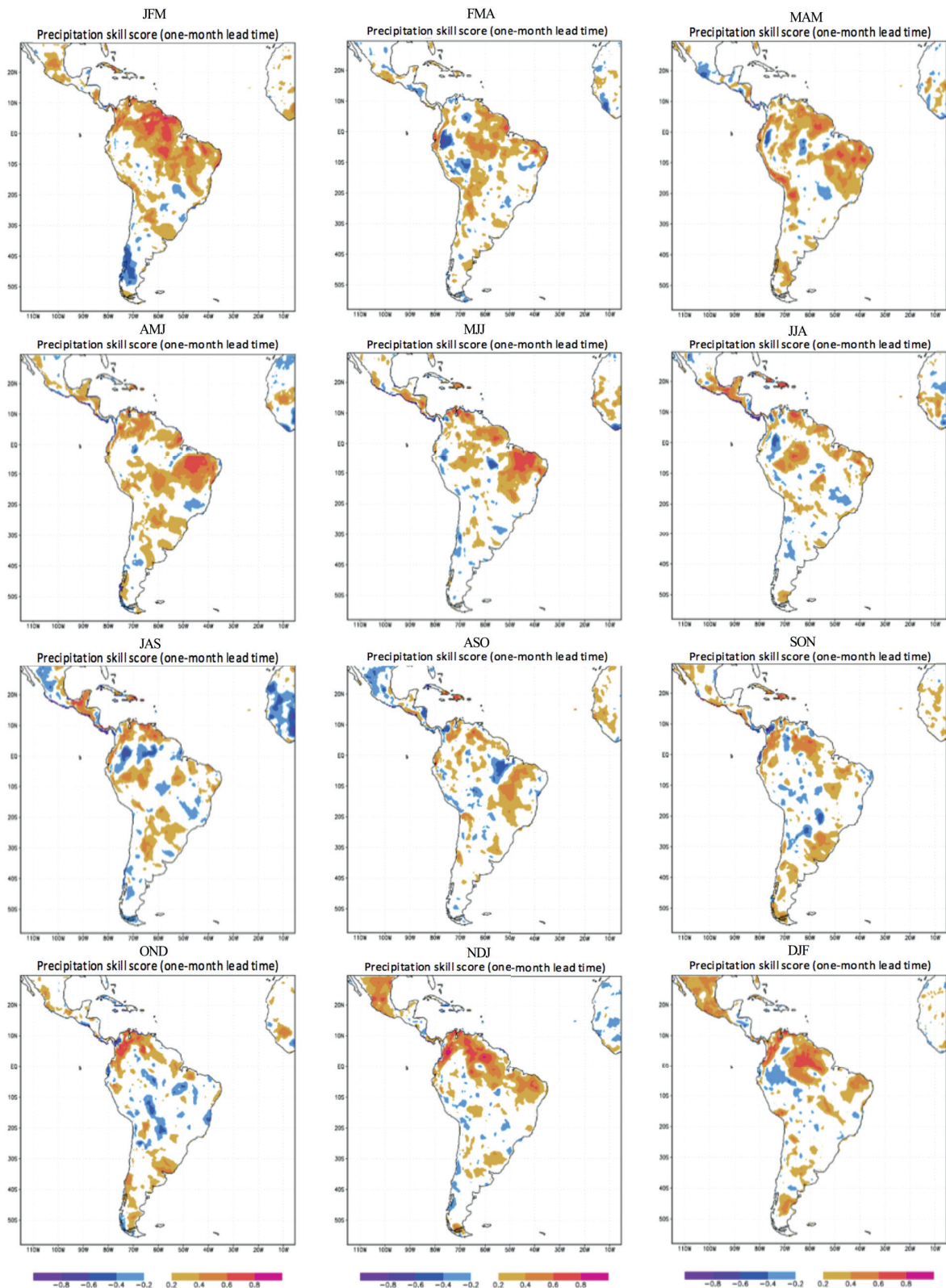
**Figure 8. Precipitation skill scores for the Eta model with one-month lead-time forecasts for the seasons: JFM, FMA, MAM, AMJ, MJJ, JJA, JAS, ASO, SON, OND, NDJ, and DJF.**
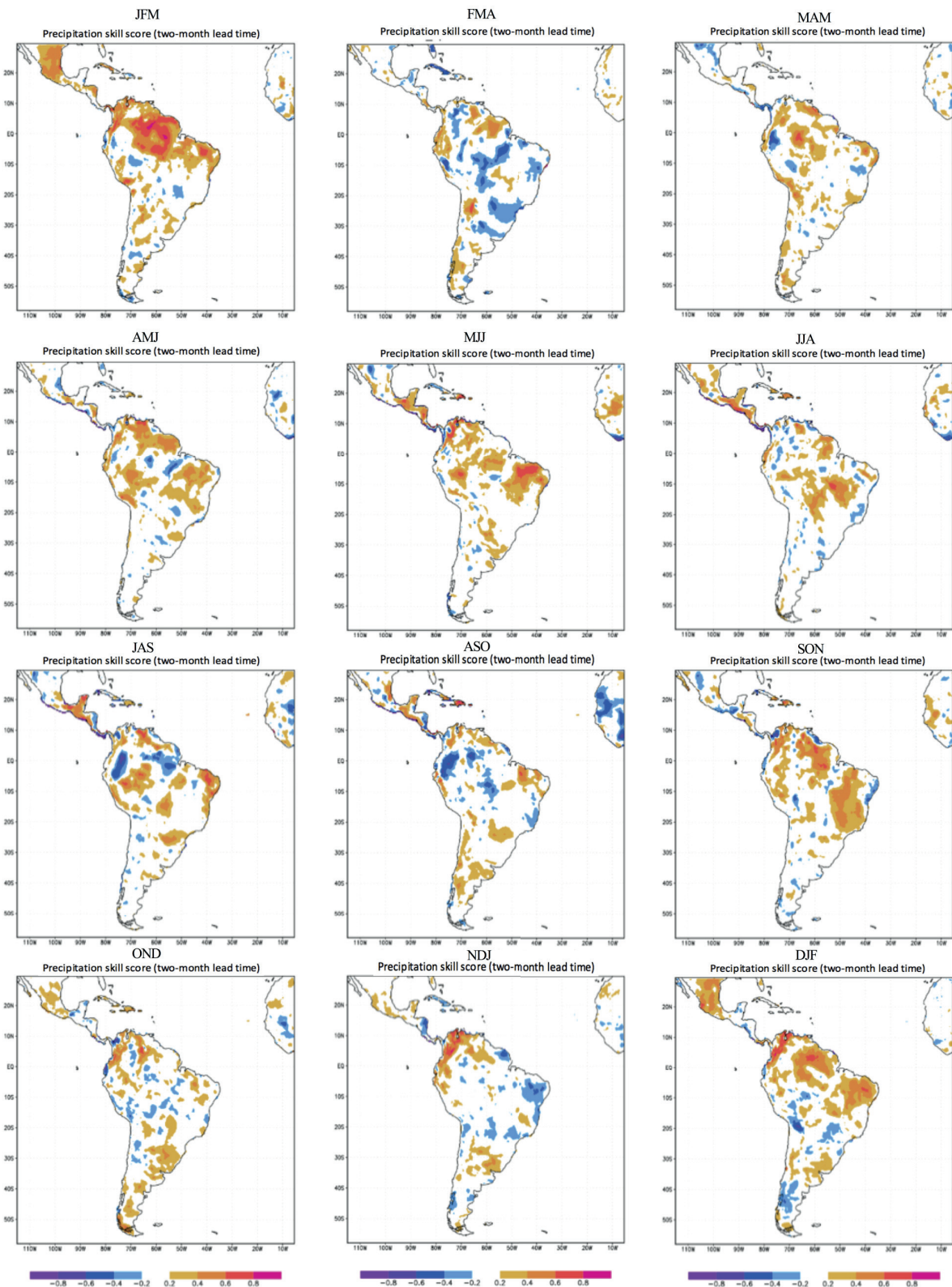
**Figure 9.** Precipitation skill scores for the Eta model with two-month lead-time forecasts for the seasons: JFM, FMA, MAM, AMJ, MJJ, JJA, JAS, ASO, SON, OND, NDJ, and DJF. The score is nondimensional.

## Extreme events

A question that arises is how well the seasonal RCM system can forecast extreme events, such as the ENSO phenomenon. Therefore, the skill scores for the El-Niño or La-Niña periods are collected and compared against the ten-year period.

The El Niño and La Niña years that occurred during the period from 2001 to 2010 are listed in Table I. This table is constructed following the information provided by NOAA's CPC: (http://www.cpc.ncep.noaa.gov/products/analysis_monitoring/ensostuff/ensoyears.shtml). Four El Niño and five La Niña events occurred but were irregularly distributed through this ten year period, indicating large climate variability.

The skill of the precipitation anomaly forecasts during events of El Niño and La Niña is crucial information to make better use of the Eta seasonal forecasts during these extreme events.

Figure 10a shows the anomaly correlation (%) values during the DJF (austral summer) season calculated using only El-Niño years. This figure shows that there are values over 80% in various parts of northeastern Brazil, where, in

**Table I.** List of El Niño and La Niña events from 2001 until 2010 (source: NOAA CPC website).

| Event | From | Until |
|---|---|---|
| El Niño | MJJ 2002 | JFM 2003 |
| | JJA 2004 | JFM 2005 |
| | ASO 2006 | DJF 2007 |
| | JJA 2009 | FMA 2010 |
| La Niña | DJF 2001 | JFM 2001 |
| | OND 2005 | FMA 2006 |
| | JJA 2007 | MJJ 2008 |
| | OND 2008 | FMA 2009 |
| | MJJ 2010 | OND 2010 |

comparison with Figure 8, the skill is not high considering the entire dataset, with values as low as approximately 20% and 40%. In addition, in the central part of Brazil, a band of relatively high skill extends from the south Amazon toward southeast Brazil, a region commonly occupied by the SACZ during DJF. This high skill band is not so clear considering the entire dataset (Figure 8). In JJA during the El Niño years (Figure 10b), higher skill scores are located in the northern part of Brazil and in northern Argentina.

Figure 10c shows the anomaly correlations (%) during FMA (autumn) calculated using only the La Niña years. The FMA season was chosen because of the strongest signal of La Niña on the continent. Skill score values that exceed 80% are found over several regions of South America, including the Amazon region, various parts of the northeastern Brazil, the Pantanal (the region between Paraguay and Brazil) and northeastern Argentina. The skill of the Eta forecasts during FMA of the La Niña years are higher than during DJF of the El Niño years, which are also higher than the skill considering the entire dataset. Therefore, the increase in predictability in the tropics due to the sea surface temperature anomaly forcing is translated into an increase in the skill of the Eta seasonal forecasts.

## Added value

In this section, we evaluate the added value of the regional climate forecasts over the driver CPTEC global atmospheric climate model forecasts. Figure 11 shows the skill score of the CPTEC global climate model (operational forecast skill at http://clima1.cptec.inpe.br/gpc/pt). One can notice that, although the global model does not exhibit strong negative skill values, it does not show strong positive skill values, either. Therefore, the skill pattern of the global model is very smooth throughout the year. The comparison of global climate model
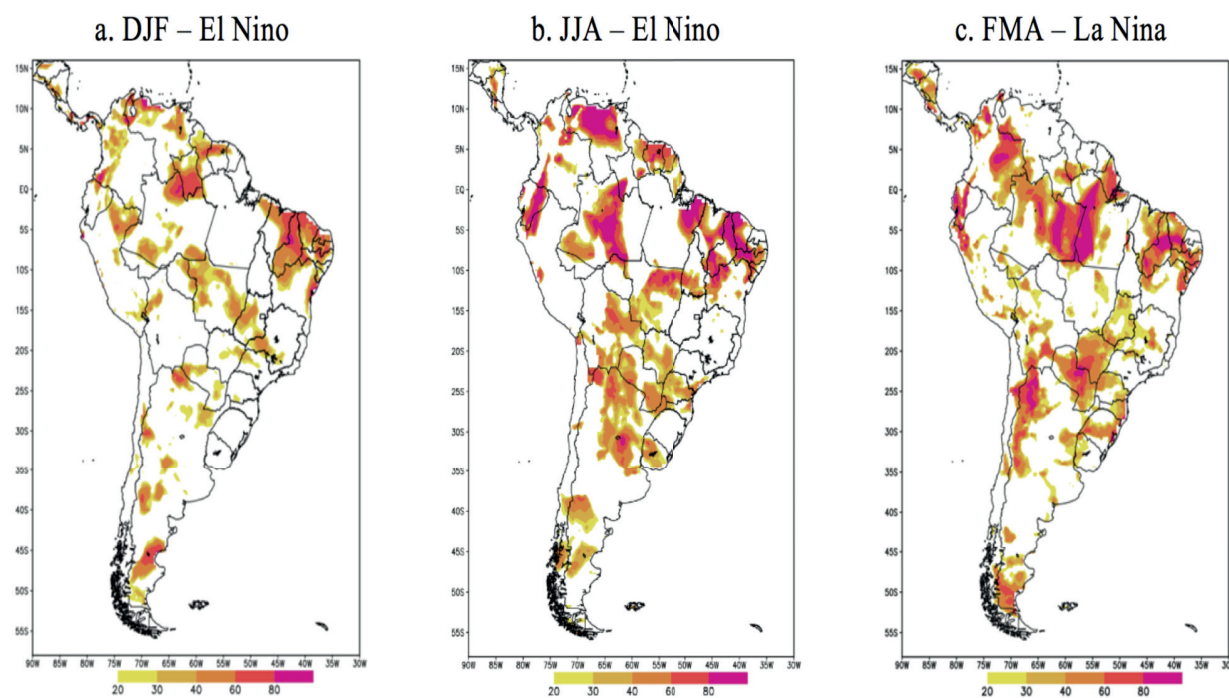
**Figure 10.** Skill scores of the seasonal precipitation anomaly (%) forecast by the Eta model with one-month lead time for DJF (a) and JJA (b) for El-Niño years; and (c) FMA of La Niña years. Only positive skill scores are shown.

forecast skill (Figure 11) against the Eta RCM forecast skill (Figure 9) shows that, although the positive skill scores are at approximately similar positions in both Eta RCM and its driver model, the Eta precipitation forecasts show higher score values, especially during the rainy seasons, but show lower score values during the winter seasons, especially in JAS.

Regardless of the extreme negative or positive values, Figure 12 highlights the areas of skill over 0.3 for both regional and global models. The seasonal forecast skill over 0.3 is considered here as the threshold for useful forecasts. In the regional model, these skill areas are very patchy, whereas in the global model, these areas are uniform. These patterns reflect the higher resolution of the regional model and the coarse resolution of the global model. Nevertheless, clearly, the downscaling by the Eta model shows additional areas of skill over 0.3 compared with

the driver global model, in particular, during the rainy seasons starting in DJF and ending in MAM.

The values of the skills of the global model are interpolated onto the same grid of the Eta model to allow a comparison to the computed areas. For an objective evaluation of the added value, the total area of skill over 0.3 is summed for both regional and global models along the year (Figure 13). Only the grid boxes over land are computed for the total area. In all seasons of the year, except in JAS and ASO, the Eta seasonal precipitation forecasts produce more areas of skill over 0.3 than the global model forecasts. During the rainy seasons of DJF and JFM, the areas of skill over 0.3 are approximately twice the total areas of the global model. An ultimate measure of the added value suggested here is the gain ratio, which is calculated as the difference of the total area of skill over 0.3 between the Eta and the global model divided by the total area of skill over 0.3 of the driver model. The
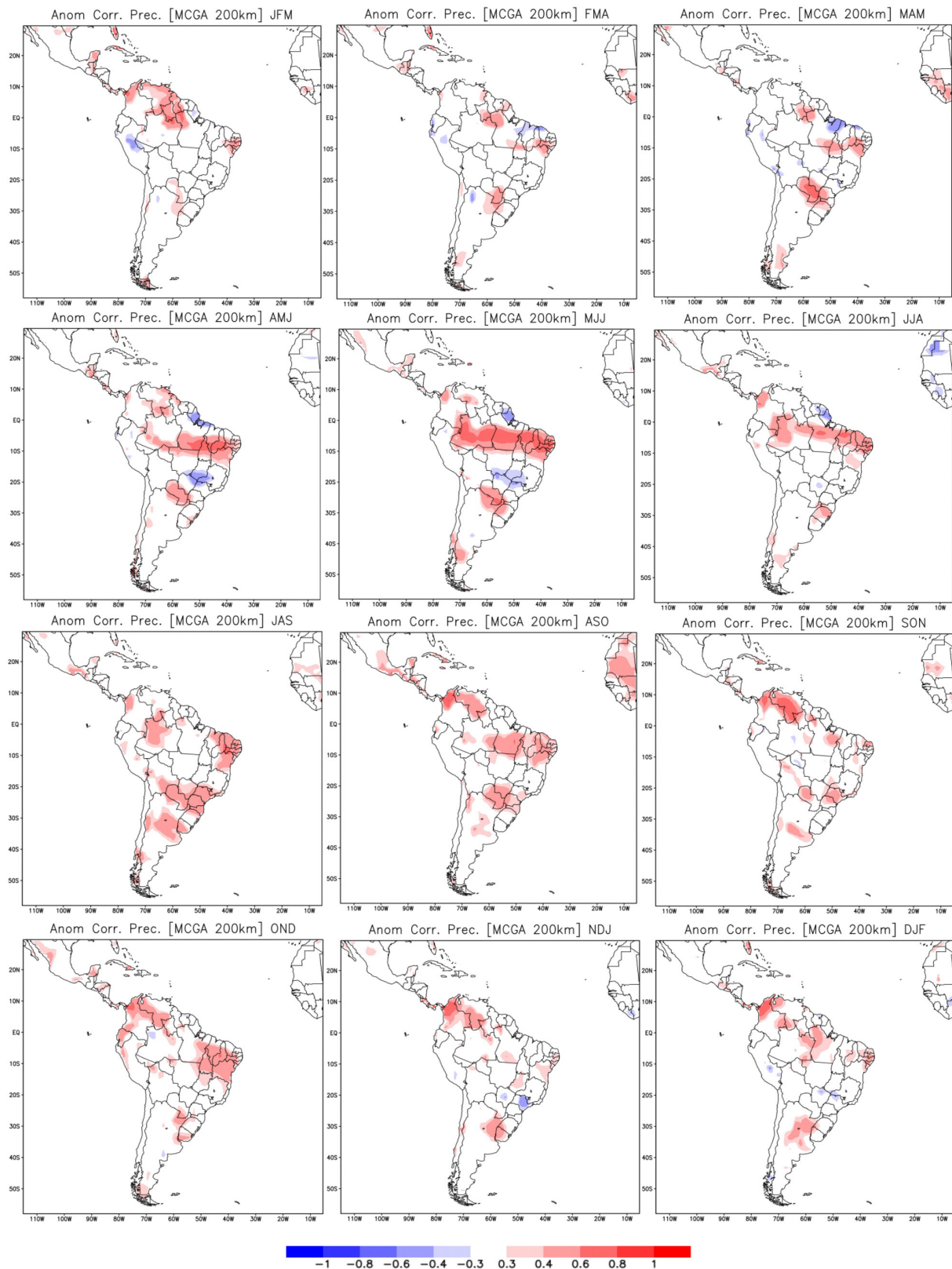
**Figure 11.** Precipitation skill scores for the CPTEC global atmospheric climate model with two-month lead time for the seasons: JFM, FMA, MAM, AMJ, MJJ, JJA, JAS, ASO, SON, OND, NDJ, and DJF. The score is nondimensional.
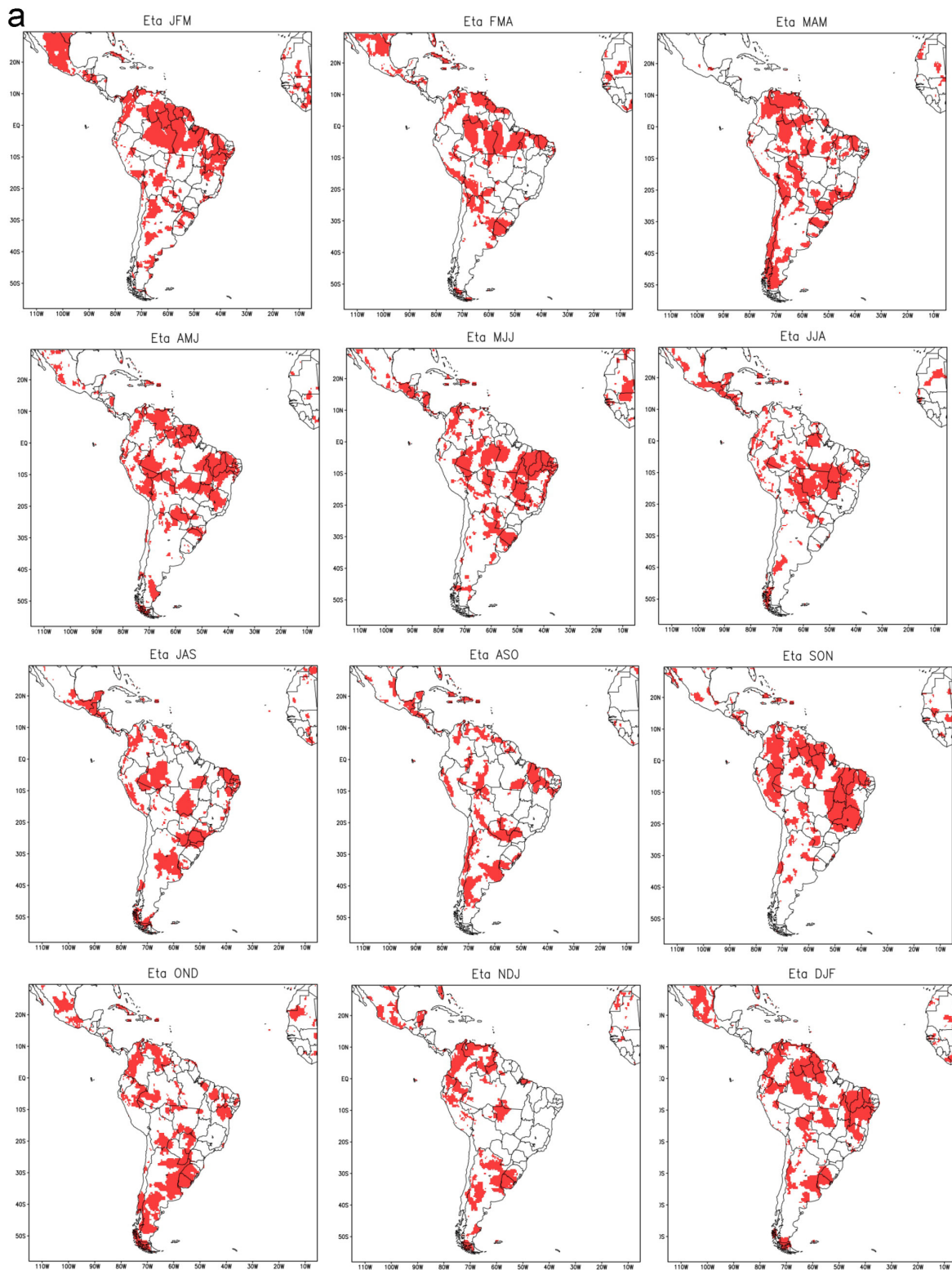
**Figure 12.** Precipitation skill scores greater than 0.3 for (a) the Eta RCM, and for (b) the CPTEC global atmospheric climate model with a two-month lead time for the seasons: JFM, FMA, MAM, AMJ, MJJ, JJA, JAS, ASO, SON, OND, NDJ, and DJF. The score is nondimensional.
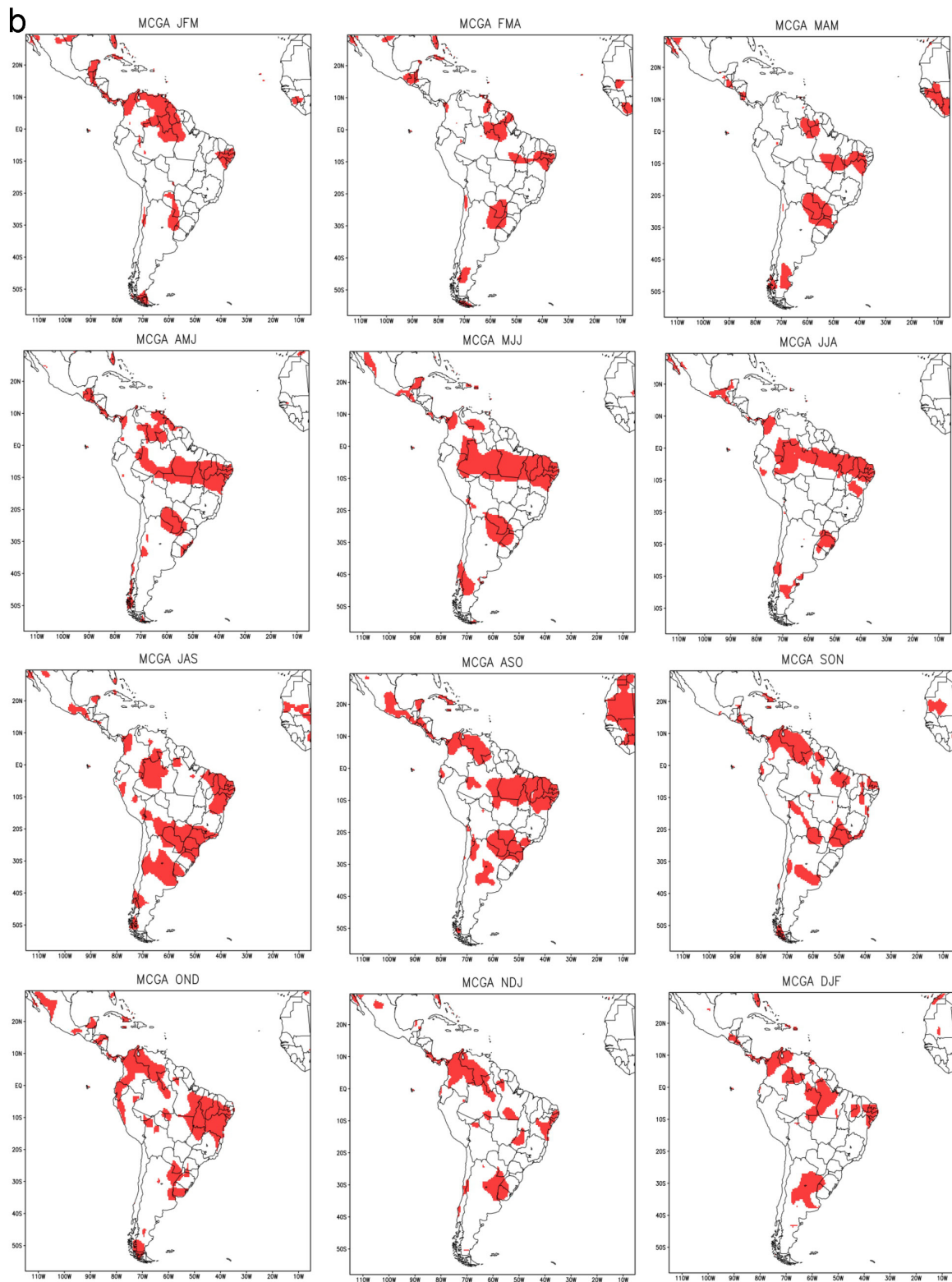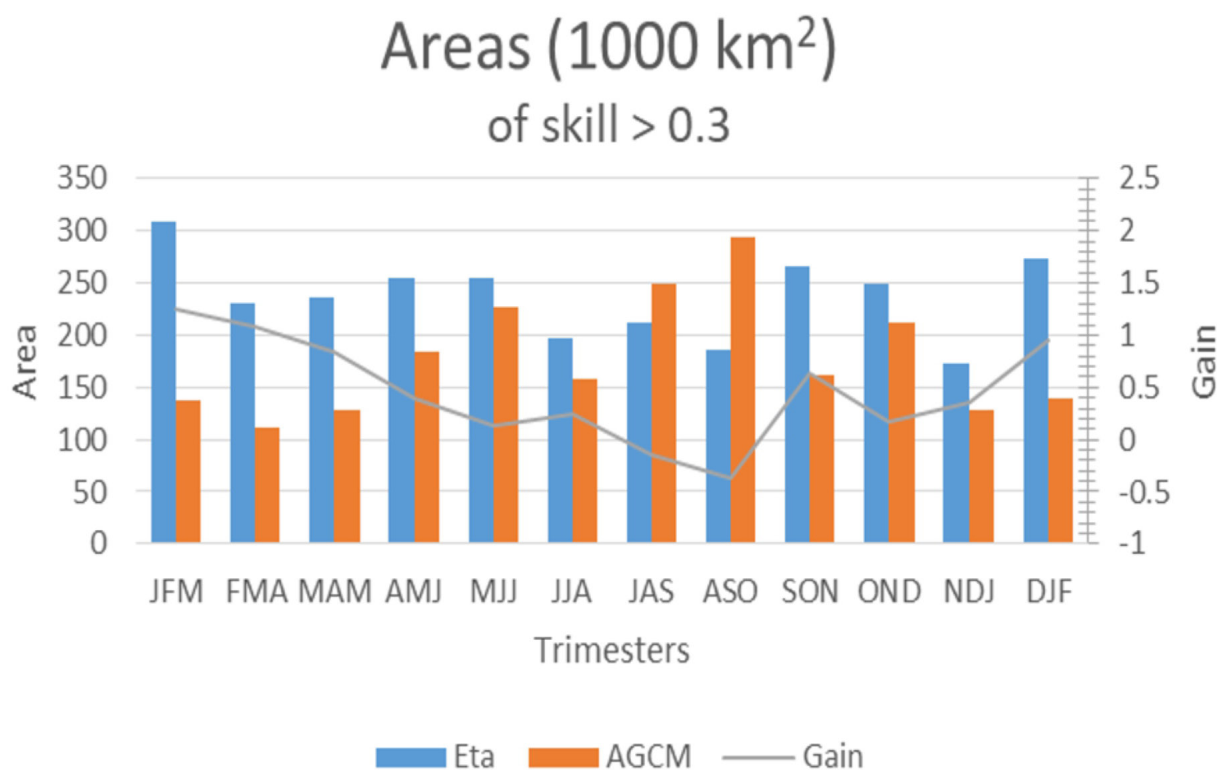
**Figure 12.** (continuation).

**Figure 13.** Total area (1000 km$^2$) where the seasonal precipitation skill score is over 0.3 for the Eta RCM (blue bars) and for the CPTEC global atmospheric climate model (red bars). The gain ratio is shown on the right axis (curve, nondimensional).

added value is indicated by the gain ratio above zero. For the seasons from DJF through MAM, the gain in skill is over 50% when using the Eta RCM over the AGCM precipitation anomaly forecasts. In addition, the SON season also exhibits approximately 50% of skill gain, which is an interesting added value to the forecast skill since the SON season is the transition between the dry and the rainy seasons in Brazil.

## CONCLUSIONS

Evaluation of ten-year seasonal reforecasts over South America produced by the Eta Regional Climate Model at 40 km resolution is shown. A five-member ensemble forecast is constructed by five consecutive dates initial conditions. Regional forecasts are driven by the CPTEC global

atmospheric model. Sea surface temperature anomalies persist during the forecast runs.

The forecasts underestimate precipitation in the central part of Brazil during summer but overestimate precipitation in the southern part of Brazil and along the eastern coast during winter. These errors in precipitation can be reduced by correcting formulations in the convection parameterization scheme of the model or by testing other parameterization schemes. Sensitivity tests are necessary to improve model precipitation production. For temperature, the major error appears to be the cold bias for most of the continent and in all runs throughout the year.

Despite the large errors in precipitation over the equatorial areas, which include the ITCZ, the precipitation scores over the northern

part of the continent show the highest skill scores. These scores indicate that the model can reproduce the interannual variability of the precipitation anomaly in these areas. In the central part of Brazil, the signs of the scores are mixed, whereas in the southern part of Brazil, weakly positive scores are exhibited. In general, the areas of higher seasonal forecast skill of the regional Eta model are very similar to the areas of the skill of the driver global atmospheric model, which agrees with the results of Seth et al. (2007). Southeastern Brazil is an area of lower seasonal forecast skill. Northern and northeastern Brazil are the areas of highest skill, whereas southern Brazil exhibits moderate skill. This skill pattern is in agreement with the skill of the driver global model (Nobre et al. 2006). The skill scores during the extreme events of El Niño and La Niña year are higher than during neutral years and are also higher compared to the global model forecasts.

The scores show that one-month lead time forecasts generally perform better than the two-month lead time forecasts. Nevertheless, operationally, by the time the forecast is issued, the two-month lead time forecasts result in a more useful forecast range.

In general, the increase in horizontal resolution by the Eta downscaling of the CPTEC global model provides added value to the seasonal forecasts over South America. This added value clearly occurs in the rainy seasons from DJF through MAM, and in the transitional season of SON. In conclusion, for the case of the Eta RCM driven by the CPTEC AGCM over South America, the benefits are two-fold: higher resolution, therefore more detailed information, and higher seasonal precipitation forecast skill.

## Acknowledgments

## REFERENCES

AMBRIZZI T, REBOITA MS, ROCHA RP & LLOPART M. 2019. The state of the art and fundamental aspects of regional climate modeling in South America. Ann N Y Acad Sci 1436: 98-120.

ANTICO PL, CHOU SC & MOURÃO C. 2017. Zonda downslope winds in the central Andes of South America in a 20-year climate simulation with the Eta model. Theor Appl Climatol 128: 291-299.

BARNSTON AG, LI S, MASON SJ, DEWITT DG, GODDARD L & GONG X. 2010. Verification of the first 11 years of IRI's seasonal climate forecasts. J Appl Meteor Climatol 49: 493-520.

BETTS AK & MILLER MJ. 1986. A new convective adjustment scheme. Part II: Single column tests using GATE wave, BOMEX, and Arctic air-mass data sets. Q J R Meteorol Soc 112: 693-709.

BLACK TL. 1994. NMC notes. The new NMC mesoscale Eta model: description and forecast examples. Wea Forecasting 9: 256-278.

BRANKOVIĆ Č, PALMER TN & FERRANTI L. 1994. Predictability of seasonal atmospheric variations. J Climate 7: 217-237.

CAVALCANTI IFA ET AL. 2002. Global climatological features in a simulation using the CPTEC-COLA AGCM. J Climate 15: 2965-2988.

CHOU SC. 1996. Modelo Regional Eta. Climanálise. Edição Comemorativa de 10 anos, INPE, São José dos Campos. http://climanalise.cptec.inpe.br/~rclimanl/boletim/cliesp10a/27.html.

CHOU SC, BUSTAMANTE J & GOMES JL. 2005. Evaluation of Eta Model seasonal precipitation forecasts over South America. Nonlin Processes in Geophys 12: 537-555.

CHOU SC, NUNES AMB & CAVALCANTI IFA. 2000. Extended range forecasts over South America using the regional Eta model. J Geophys Res 105: 10147-10160.

CHOU SC, TANAJURA CAS, XUE Y & NOBRE CA. 2002. Validation of the Coupled Eta/SSiB Model over South America. J Geophys Res 107(D20 8088).

CHOU SC ET AL. 2012. Downscaling of South America present climate driven by 4-member HadCM3 runs. Clim Dyn 38: 635-653.

CHOU SC ET AL. 2014. Evaluation of the Eta Simulations Nested in Three Global Climate Models. Am J Climate Change 3: 438-454.

COELHO CAS, STEPHENSON DB, BALMASEDA M, DOBLAS-REYES FJ & OLDENBORGH GJV. 2006. Towards an integrated seasonal forecasting system for South America. J Climate 19: 3704-3721.

DEE DP ET AL. 2011. The ERA-Interim reanalysis: Configuration and performance of the data assimilation system. Q J R Meteorol Soc 137: 553-597.

DICKINSON RE, ERRICO RM, GIORGI F & BATES GT. 1989. A regional climate model for the western United States. Climatic Change 15: 383-422.

EK MB, MITCHELL KE, LIN Y, ROGERS E, GRUMMEN P, KOREN V, GAYNO G & TARPLEY JD. 2003. Implementation of NOAH land surface advances in the National Centers for Environmental Prediction operational mesoscale Eta model. J Geophys Res 108: D22-D8851.

FERREIRA NCR & CHOU SC. 2018. Influence of Soil Texture Type and Initial Soil Moisture on the Simulation of Seasonal Precipitation and Extreme Precipitation in Southeast Brazil. Anu Inst Geocienc 41: 680-689.

GIORGI F. 1990. Simulation of regional climate using a limited area model nested in a general circulation model. J Climate 3: 941-963.

HAMILL TM. 2012. Verification of TIGGE multimodel and ECMWF reforecast-calibrated probabilistic precipitation forecasts over the contiguous United States. Mon Wea Rev140(7): 2232-2252.

HAMILL TM, WHITAKER JS & WEI X. 2004. Ensemble forecasting: Improving medium-range forecast skill using retrospective forecasts. Mon Wea Rev 132(6): 1434-1447.

HUFFMAN GJ, ADLER RF, ARKIN P, CHANG A, FERRARO R, GRUBER A, JANOWIAK J, MCNAB A, RUDOLF B & SCHNEIDER U. 1997. The global precipitation climatology project (GPCP) combined precipitation dataset. Bull Amer Meteor Soc 78(1): 5-20.

JANJIC ZI. 1979. Forward-backward scheme modified to prevent two grid-interval noise and its application in σ coordinate models. Contrib Atmos Phys 52: 69-84.

JANJIC ZI. 1984. Nonlinear advection schemes and energy cascade on semi-staggered grids. Mon Wea Rev 112: 1234-1245.

JANJIC ZI. 1994. The step-mountain eta coordinate model: Further developments of the convection, viscous sublayer, and turbulence closure schemes. Mon Wea Rev 122: 927-945.

KODAMA YM. 1992. Large-scale common features of sub-tropical precipitation zones (the Baiu Frontal Zone, the SPCZ, and the SACZ). Part I: characteristics of subtropical frontal zones. Journal of the Meteorological Society of Japan 70: 813-835.

KOUSKY VE & GAN AM. 1981. Upper tropospheric cyclonic vortices in the tropical South Atlantic. Tellus 33: 538-551.

KUMAR A. 2007. On the Interpretation and Utility of Skill Information for Seasonal Climate Predictions. Mon Wea Rev 135: 1974-1984.

KUMAR A, JHA B, ZHANG Q & BOUNOUA L. 2007. A new methodology for estimating the unpredictable component of seasonal atmospheric variability. J Climate 20: 3888-3901.

LACIS AA & HANSEN JE. 1974. A parameterization of the absorption of solar radiation in the earth's atmosphere. J Atmos Sci 31: 118-133.

LAPRISE R, ELÍA R, CAYA D, BINER S, LUCAS-PICHER P, DIACONESCU E, LEDUC M, ALEXANDRU A & SEPAROVIC L. 2008. Challenging some tenets of regional climate modelling. Meteorol Atmos Phys 100: 3-22.

LAPRISE R, VARMA MR, DENIS B, CAYA D & ZAWADZKI I. 2000. Predictability of a nested limited-area model. Mon Wea Rev 128: 4149-4154.

LIANG XZ, PAN J, ZHU J, KUNKEL KE, WANG JX & DAI A. 2006. Regional climate model downscaling of the US summer climate and future change. J Geophys Res Atmospheres 111(D10).

LORENZ EN. 1982. Atmospheric predictability experiments with a large numerical model. Tellus 34: 505-513.

MENÉNDEZ CG, SAULO AC & LI ZX. 2001. Simulation of South American wintertime climate with a nesting system. Climate Dynamics 17: 219-231.

MESINGER F. 1977. Forward-backward scheme, and its use in a limited area model. Contrib Atmos Phys 50: 200-210.

MESINGER F. 1984. A blocking technique for representation of mountains in atmospheric models. Riv Meteorol Aeronautica 44: 195-202.

MESINGER F, JANJIC ZI, NICKOVIC S, GAVRILOV D & DEAVEN DG. 1988. The step-mountain coordinate: model description, and performance for cases of Alpine lee cyclogenesis and for a case of an Appalachian redevelopment. Mon Wea Rev 116:1493–1518.

MESINGER F ET AL. 2012. An upgraded version of the Eta model. Meteorology and Atmospheric Physics 116: 63-79.

MISRA V, DIRMEYER PA & KIRTMAN BP. 2003. Dynamic downscaling of seasonal simulations over South America. J Climate 16: 103-117.

MISRA V, DIRMEYER PA, KIRTMAN BP, JUANG HMH & KANAMITSU M. 2002. Regional simulation of interannual variability over South America. J Geophys Res: Atmospheres 107(D20).

MITCHELL TD & JONES PD. 2005. An Improved Method of Constructing a Database of Monthly Climate Observations and Associated High-Resolution Grids. Int J Climatol 25: 693-712.

NICOLINI M, SALIO P, KATZFEY JJ, MCGREGOR JL & SAULO AC. 2002. January and July regional climate simulation over South America. J Geophys Res: Atmospheres 107(D22).

NOBRE P, MARENGO JA, CAVALCANTI IFA, OBREGON G, BARROS V, CAMILLONI I, CAMPOS N & FERREIRA AG. 2006. Seasonal-to-decadal predictability and prediction of South American climate. J Climate 19: 5988-6004.

OTTO FE ET AL. 2015. Factors other than climate change, main drivers of 2014/15 water shortage in southeast Brazil. Bull Amer Meteor Soc 96: S35-S40.

PALMER TN & ANDERSON DL. 1994. The prospects for seasonal forecasting—A review paper. Q J R Meteorol Soc 120: 755-793.

PAULSON CA. 1970. The mathematical representation of wind speed and temperature profiles in the unstable atmospheric surface layer. J App Meteorol 9: 857-861.

PEGION K & KUMAR A. 2013. Does an ENSO-conditional skill mask improve seasonal predictions? Mon Wea Rev 141: 4515-4533.

PESQUERO JF, CHOU SC, NOBRE CA & MARENGO JA. 2009. Climate downscaling over South America for 1961-1970 using the Eta Model. Theor Appl Climatol 99: 75-93.

PILOTTO ID, CHOU SC & NOBRE P. 2012. Seasonal climate hindcasts with Eta model nested in CPTEC coupled ocean-atmosphere general circulation model. Theor Appl Climatol 110: 437-456.

RAJAGOPALAN B, LALL U & ZEBIAK SE. 2002. Categorical climate forecasts through regularization and optimal combination of multiple GCM ensembles. Mon Wea Rev 130: 1792-1811.

RESENDE N & CHOU SC. 2015. Influência das condições do solo na climatologia da previsão sazonal do modelo Eta. Rev Bras Climatol 15: 64-79.

RODWELL MJ & DOBLAS-REYES FJ. 2006. Medium-range, monthly, and seasonal prediction for Europe and the use of forecast information. J Climate 19: 6025-6046.

SAHA S ET AL. 2010. The NCEP Climate Forecast System Reanalysis. Bull Amer Meteor Soc 91: 1015-1058.

SATYAMURTY P, NOBRE C & SILVA DIAS PL. 1988. South America. In: Karoly DJ & Vincent DG (Eds), Meteorology of the Southern Hemisphere. Meteorological Monographs. American Meteorological Society, Boston, MA.

SCHWARZKOPF MD & FELS SB. 1991. The simplified exchange method revisited: an accurate, rapid method for computation of infrared cooling rates and fluxes. J Geophys Res 96: 9075–9096.

SELUCHI ME, NORTE F, SATYAMURTY P & CHOU SC. 2003. Analysis of three situations of foehn effect over the Andes. Wea Forecasting 18: 481-501.

SETH A, RAUSCHER SA, CAMARGO SJ, QIAN JH & PAL JS. 2007. RegCM3 regional climatologies for South America using reanalysis and ECHAM global model driving fields. Clim Dyn 28: 461-480.

SHUKLA J. 1998. Predictability in the midst of chaos: A scientific basis for climate forecasting. Science 282: 728-731.

SHUKLA J ET AL. 2000. Dynamical seasonal prediction. Bull Amer Meteor Soc 81: 2593-2606.

SOORAJ KP, ANNAMALAI H, KUMAR A & WANG H. 2012. A comprehensive assessment of CFS seasonal forecasts over the tropics. Wea Forecasting 27: 3-27.

STEFANOVA L & KRISHNAMURTI TN. 2002. Interpretation of seasonal climate forecast using Brier skill score, the Florida State University superensemble, and the AMIP-I dataset. J Climate 15: 537-544.

STERN W & MIYAKODA K. 1995. Feasibility of seasonal forecasts inferred from multiple GCM simulations. J Climate 8: 1071-1085.

YAMAZAKI Y & RAO VB. 1977. Tropical cloudiness over the South Atlantic Ocean. Journal of the Meteorological Society of Japan 55: 205-207.

ZHAO Q, BLACK TL & BALDWIN ME. 1997. Implementation of the cloud prediction scheme in the Eta model at NCEP. Wea Forecasting 12: 697-712.

**SIN CHAN CHOU**[1]
https://orcid.org/0000-0002-8973-1808

**CLAUDINE DERECZYNSKI**[2]
https://orcid.org/0000-0002-9394-1832

**JORGE LUÍS GOMES**[1]
https://orcid.org/0000-0003-2235-171X

**JOSÉ FERNANDO PESQUERO**[1]
https://orcid.org/0000-0002-4561-7624

**ANA MARIA H. DE AVILA**[3]
https://orcid.org/0000-0002-6801-8528

**NICOLE C. RESENDE**[1]
https://orcid.org/0000-0002-3098-5993

**LUÍS FELIPE ALVES DE CARVALHO**[1]
https://orcid.org/0000-0002-4470-6334

**RAMIRO RUIZ-CÁRDENAS**[4]
https://orcid.org/0000-0002-2391-4134

**CARLOS RENATO DE SOUZA**[1]
https://orcid.org/0000-0002-4022-9382

**JOSIANE FERREIRA F. BUSTAMANTE**[†]

[1]National Institute for Space Research (INPE), Rodovia Pres. Dutra, Km 39, 12630-000 Cachoeira Paulista, SP, Brazil

[2]Federal University of Rio de Janeiro (UFRJ). Av. Athos da Silveira Ramos, 274, 21941-916 Rio de Janeiro, RJ, Brazil

[3]University of Campinas (UNICAMP), Cidade Universitária "Zeferino Vaz", s/n, 13083-970 Campinas, SP, Brazil

[4]Rua Alexandre Siqueira 275/1201, Caiçara, 30775-540 Belo Horizonte, MG, Brazil

**†***In memorian*

Correspondence to: **Sin Chan Chou**
*E-mail: chou.chan@inpe.br*

## Author Contributions

Sin Chan Chou: Conceptualization, formal analysis, writing, supervision. Claudine Dereczynski: Writing, formal analysis. Jorge Luís Gomes: Methodology, data curation, writing. José Fernando Pesquero: Dataprocessing, data curation. Ana Maria Heuminski de Avila, Nicole Costa Resende, Luís Felipe Alves de Carvalho, Ramiro Ruiz-Cárdenas, Carlos Renato de Souza, Josiane Ferreira F. Bustamante: Data processing, analysis.